JSES International 8 (2024) 880–887

Contents lists available at ScienceDirect

JSES International

journal homepage: www.jsesinternational.org

Stemless reverse shoulder arthroplasty neck shaft angle influences humeral component time-zero fixation and survivorship: a cadaveric biomechanical assessment

David E. Cunningham, PhD[a,b], Ahmed A. Habis, MD, MSc, FRCSC[c,b,d], Fares Z.N. Uddin, MD, MRCSI, SB-ORTH[e,b,d], James A. Johnson, PhD[a,b,d,f], George S. Athwal, MD, FRCSC[b,d,*]

[a]Department of Mechanical Engineering, The University of Western Ontario, London, ON, Canada
[b]The Roth|McFarlane Hand and Upper Limb Centre, St. Joseph's Hospital, London, ON, Canada
[c]Faculty of Medicine, Department of Orthopaedic Surgery, King Abdulaziz University, Jeddah, Saudi Arabia
[d]Department of Surgery, The University of Western Ontario, London, ON, Canada
[e]Orthopedic Department, Bahrain Royal Guard/King Hamad University Hospital, Royal Medical Services-Bahrain, Defence Force, Al Sayh, Bahrain
[f]Department of Biomedical Engineering, The University of Western Ontario, London, ON, Canada

ARTICLE INFO

Keywords:
Stemless
Neck shaft angle
Arthroplasty
Implant design
Reverse shoulder arthroplasty
Cuff tear arthropathy
Implant micromotion

Level of evidence: Basic Science Study; Biomechanics

Background: Stemless humeral components are being clinically investigated for reverse shoulder arthroplasty (RSA) procedures. There is, however, a paucity of basic science literature on the surgical parameters that influence the success of these procedures. Therefore, this cadaveric biomechanical study evaluated the neck shaft angle (NSA) of implantation on the survivability and performance of stemless RSA humeral components during cyclical loading.

Methods: Twelve paired cadaveric humeri were implanted with stemless RSA humeral components at NSAs of 135° and 145°. Implant–bone motion at the periphery of the implant was measured with 3 optical machine vision USB3 cameras outfitted with c-mount premium lenses and quantified with ProAnalyst software. A custom 3-dimensional loading apparatus was used to cyclically apply 3 loading directions representative of physiological states at 5 progressively increasing loading magnitudes. Stemless 135° and 145° implants were compared based on the maximum implant–bone relative distraction detected, as well as the survivorship of the implants throughout the loading protocol.

Results: Primary fixation and implant biomechanical survivorship were substantially better in the 145° NSA implants. The 135° NSA implants elicited significantly higher implant–bone distractions during cyclical loading ($P = .001$), and implant survivorship was considerably lower in the 135° NSA specimens when compared to the 145° NSA specimens (135° NSA: 0%, 145° NSA: 50%) ($P < .001$).

Conclusion: NSA is a modifiable parameter that influences time-zero implant stability, as well as the early survivorship of the stemless RSA humeral components tested in this study. NSA resections of 145° appear to promote better stability than those utilizing 135° NSAs during early postoperative eccentric loads. Further studies are required to assess if other stemless reversed humeral implant designs have improved time-zero fixation at higher NSAs.

In the recent years, stemless reverse shoulder arthroplasty (RSA) humeral prostheses have been introduced to preserve healthy bone stock, to minimize periprosthetic humeral fractures, and to simplify future revision surgeries.[9,17] Additionally, these shorter humeral implants have been shown to better-mimic the natural force-transmission properties of the shoulder joint, thereby reducing risk of stress shielding in periprosthetic bone.[18] However, stemless humeral implants rely primarily on metaphyseal bone press-fit for stability and fixation, and are therefore vulnerable to poor initial fixation or loosening depending on implantation and/or metaphyseal bone properties and morphology,[17] which often may be compromised by disuse osteopenia or osteoporosis.[5]

Investigations performed at the Roth|McFarlane Hand and Upper Limb Center, London, Ontario, Canada.

Institutional review board approval was not required for this study.

*Corresponding author: George S. Athwal, MD, FRCSC, Roth | McFarlane Hand & Upper Limb Centre, 268 Grosvenor Street, London, ON, Canada.
E-mail address: gsathwal@hotmail.com (G.S. Athwal).

https://doi.org/10.1016/j.jseint.2024.04.001

Surgeons must decide on the surgical variable of resection inclination (or neck shaft angle (NSA)) of the humeral head. Currently, most standard RSA systems vary the NSA between 135° to 155°. Previously, it has been reported that decreasing NSA may reduce the risk of scapular notching,[13] and may increase total impingement-free range of motion.[13] With respect to implant fixation, a recent computational finite element study reported that decreasing NSA may also significantly decrease the initial fixation of stemless RSA humeral components, potentially leading to increased incidence of premature failure in these implants.[5] This was commensurate to the results of a previous retrospective clinical study, which found that in a small series RSA humeral component loosening was more prevalent in 135° NSA-stemmed implants when compared to 155° NSA-stemmed implants[12]; although the data were not statistically significant due to the small numbers. As present, there are little clinical data available on failure modes of stemless RSA implants.

Currently, no in vitro studies are available that have evaluated the effect of NSA in stemless RSA humeral components during physiological loading. This present investigation compared 135° and 145° NSA stemless RSA humeral component performance and its effect on primary implant stability and early survivorship. We hypothesized that humeral components implanted at 145° NSA would exhibit better primary biomechanical stability and improved implant survivorship when compared to those implanted at 135° NSA.

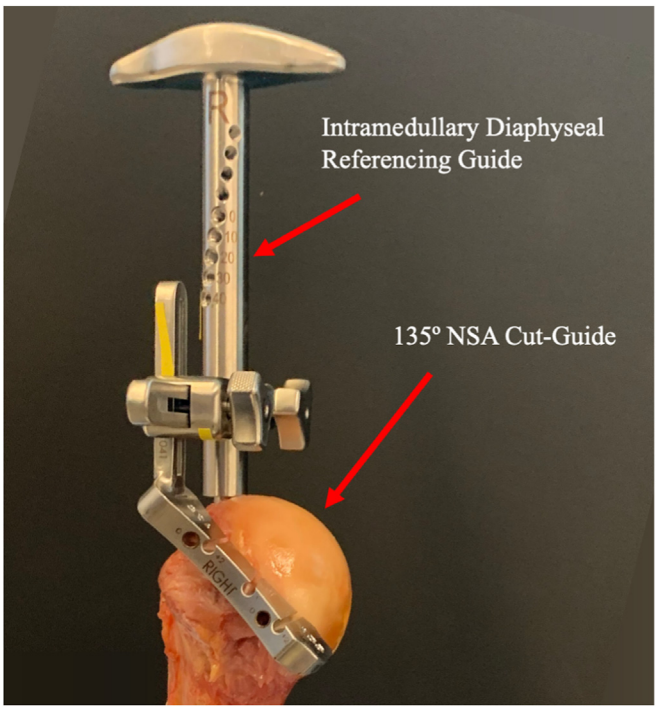

Figure 1 NSA cut guide: depicting the intermedullary diaphyseal referencing guide and 135° NSA cut-guide attachment. *NSA*, neck shaft angle.

Methods

Specimen preparation

Twelve paired cadaveric shoulder specimens (height: 171 ± 4 cm, weight: 57 ± 20 kg) aged 57 ± 12 years (mean ± standard deviation) were implanted with metaphyseal filling 2-tiered round stemless RSA humeral components (Tornier Perform® Stemless Reverse Humeral System, Stryker, Kalamazoo, MI, USA) by 3 board-certified orthopedic surgeons (GSA, AH, FU). The implant evaluated was of press-fit design, with a combination of 3D-printed and plasma-sprayed titanium surface finishes. Nominal barrel and fin interferences of 1.5 mm and 0.75 mm were present, respectively. The bone mineral density of the local periprosthetic bone was calculated using a clinical CT Scanner (GE 750HD Discovery Scanner; GE Healthcare, Chicago, IL, USA) and cortical bone surrogate (SB3 model 450; GAMMEX, Middleton, WI, USA) and distilled water phantoms. The average periprosthetic bone mineral density of the specimens evaluated was 0.106 ± 0.003 g/mm^3.

Each bilateral specimen pair (L/R) was randomized to receive a 135° NSA and a 145° NSA implantation, and a single surgeon positioned both components in each pair. Each NSA cut was prepared using an intramedullary diaphyseal referencing cut-guide (Fig. 1). Two stemless reverse humeral implant sizes were utilized, sized based on individual patient geometry. A constant size was utilized between each bilateral 135°/145° NSA pair to remove the independent variable of sizing. After the humeral head resection, the metaphyseal bone was reamed with an appropriately sized reamer, followed by insertion of the stemless trial implant. After that, the trial implant was removed and the final implant was impacted in and press-fit into the prepared humerus.

In vitro loading protocol

A custom loading apparatus (Fig. 2) was used to apply 3 loading conditions representative of aggressive boundary loading (extreme physiological loads) that a humeral implant might reasonably experience in the early postoperative period. This boundary loading envelope was calculated to represent the 95% percentile of all the relevant loads from instrumented humeral implants that were available on the OrthoLoad database[6] (Fig. 3)—a database with records of the articular forces generated from telemetrized humeral implants during common upper limb motions. This envelope was developed by plotting all relevant articular load vectors into the humeral coordinate system, then establishing limits based on the upper and lower values ± 2 standard deviations from the mean in a spherical coordinate system.

Loads with vectors pointed most superior-inferiorly were predominantly 90° abduction motions, whereas loads with vectors pointed most anterior-posteriorly included steering a steering wheel or arm elevation motions. Most OrthoLoad[6] loads were directed along the anterosuperior—posteroinferior vector direction. These included combing hair, 2-kg waist-height lifting, and some elevation and abduction motions.[6] Loads with the largest magnitude/eccentricity combination, and therefore most challenging to implant fixation, included a 2-kg head-height lifting motion, a single-hand steering motion, and an unweighted 90° abduction motion. The aforementioned boundary loads were reconverted into the humeral coordinate system for load application (Fig. 4). For each trial, the order of loading direction was randomized. Each loading set (Superior, Anterosuperior, and Anterior) was applied for 30 cycles at a frequency of 1 Hz at 20%, 40%, 60%, 80%, and 100% of the physiological magnitude.

Measurement of implant stability

Implant—bone micromotion (ie, implant distraction orthogonal to the bone surface) was used as the primary outcome. Three optical machine vision USB3 cameras (acA4096-30uc, Basler AG, Ahrensburg, SH, Germany) were outfitted with c-mount premium lenses (FL-BC3518-9M, Ricoh, Tokyo, Kanto, Japan) (resultant pixel size of 3.45 μm) and focused on the implant—bone interface to collect micromotion measurements at the superior, anterosuperior,

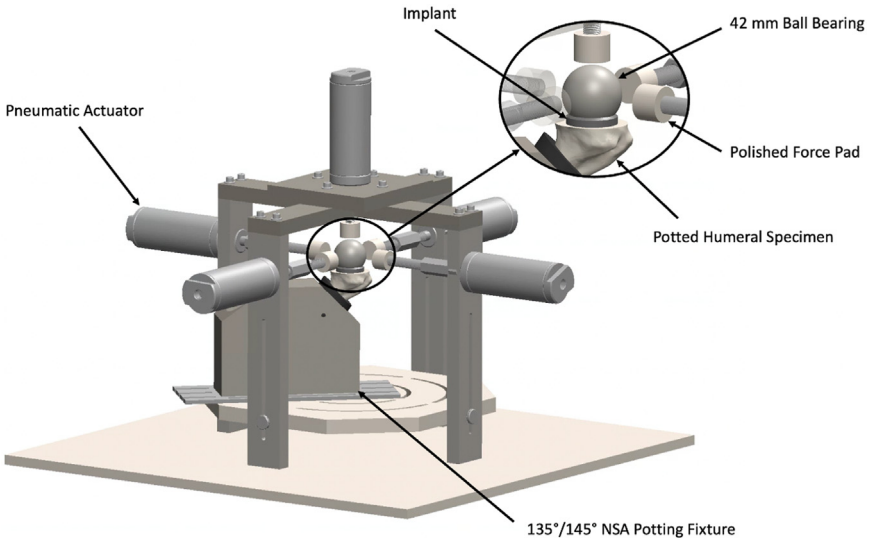

Figure 2 A custom 3-dimensional loading apparatus used to apply physiological loads to a stemless humeral RSA implant. For the purposes of the figure, a 135° NSA specimen has been positioned for loading. Loads were applied using an array of (5) pneumatic actuators, which articulated pistons with polished force pads. Combinates of loads on each actuator applied resolved physiological loads to the 42-mm ball bearing, which was utilized as a proxy for the glenosphere component of the reversed total shoulder arthroplasty. The potted humeral specimen was positioned using a custom adaptable potting fixture to facilitate a static boundary condition during loading. *CT*, computed tomography; *RSA*, reverse shoulder arthroplasty; *NSA*, neck shaft angle.

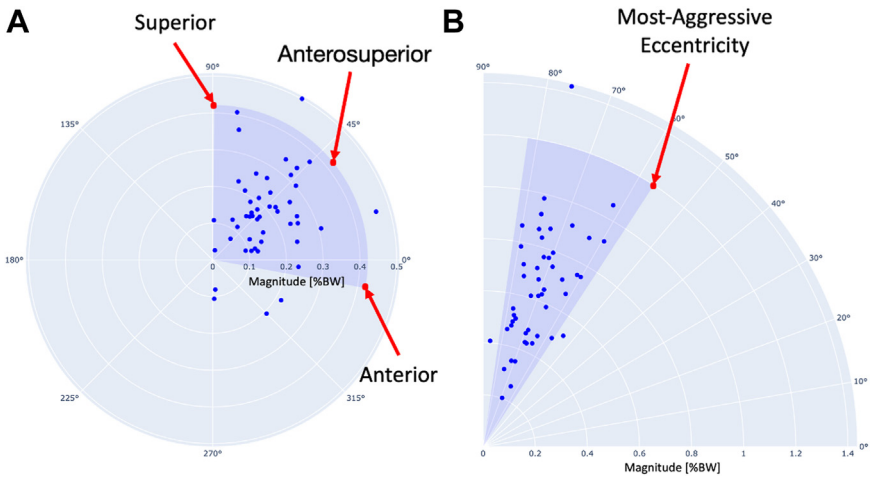

Figure 3 Scatter plots of relevant OrthoLoad[6] load vectors relative to the local resection coordinate system. (**A**) represents a summary of all vector tails orthogonal to the resection plane, whereas (**B**) indicates the relevant loads' eccentricities relative to the resection plane. The superior, anterosuperior, and anterior simulated loads are indicated by the (↑) and (●). All loading directions were evaluated at the most aggressive eccentricity experienced to simulate the most challenging loading profile to implant stability.

and anterior edges of each implant (Fig. 5). Micromotion data were extracted from the collected high-resolution digital images using ProAnalyst (Xcitex Inc., Woburn, MA, USA) motion analysis software. All images were collected and stored in Tagged Image File Format (.TIFF). Implant survivability (defined as maximum micromotion of less than 350 μm during the cyclical test), was used as the secondary outcome measure for this study. A limit of 350 μm was utilized, as this was the observed threshold of micromotion before critical macrofailure of the bone or disassociation of the implant occurred.

Statistical analyses

A 2-way paired repeated measures analysis of variance was conducted for the dependent variables of NSA and loading scenario, and a 1-way paired repeated measures analysis of variance was conducted for the dependent variable of survivability. All statistical analyses were computed using SciPy 1.9.1[23], with the threshold of significance set at $P < .05$ and Bonferroni correction with an adjusted alpha level of 0.025 (0.05/2) per 2-way test.

Results

At a 145° NSA, all implants experienced significantly lower time-zero micromotions ($P = .001$) and increased survivorship ($P < .001$) when compared to the 135° NSA implantations. For all loading scenarios, maximum micromotion was detected on the implant edge that was opposite to the direction of loading. Micromotions detected were significantly higher in the 135° NSA implantations (Table I)($P = .001$) (Fig. 6), and the catastrophic failure rate was also

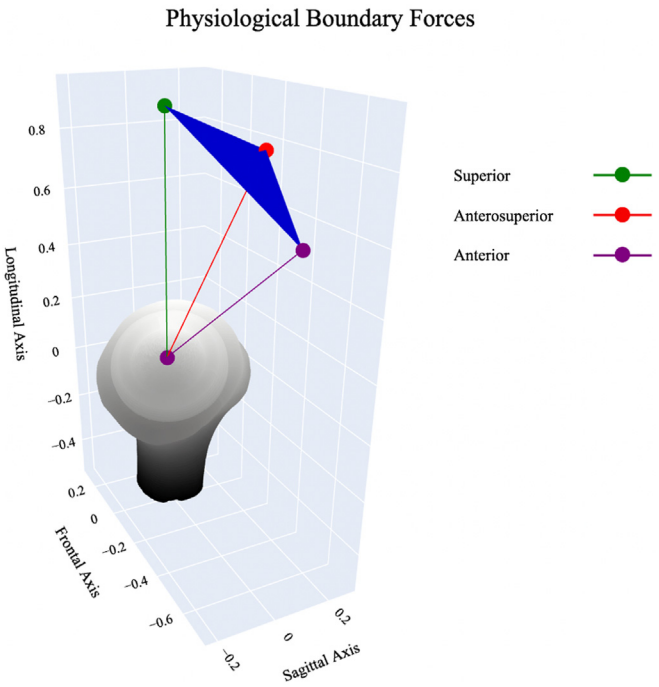

Figure 4 Boundary loads representing 95% of loading scenarios available on the OrthoLoad[6] database. The humerus represented in the figure is a Left side specimen resected at 135° NSA. *NSA*, neck shaft angle.

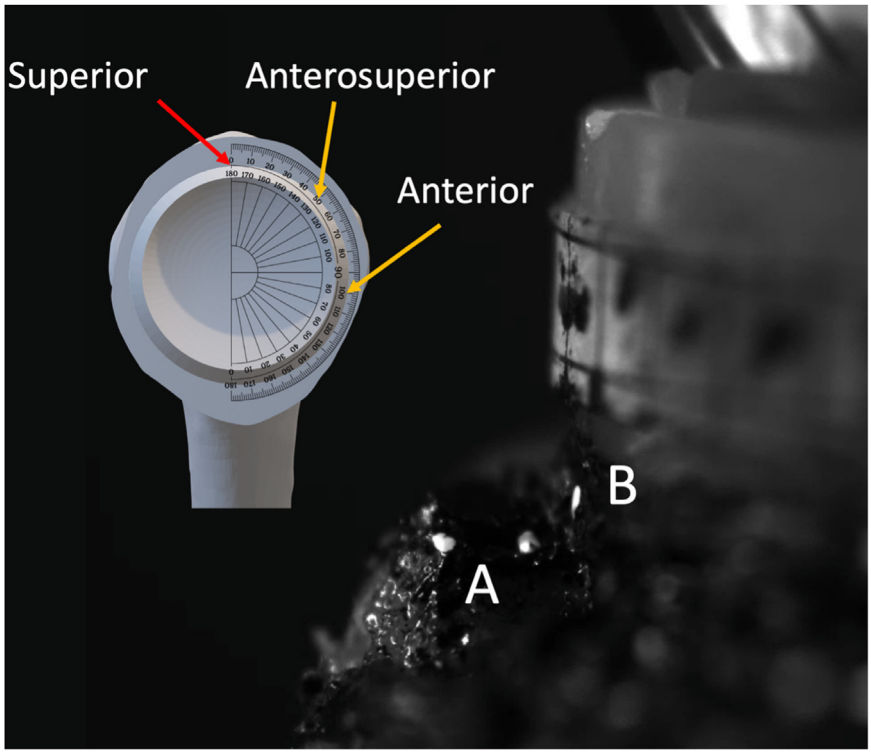

Figure 5 A high-resolution image of the implant–bone interface on the superior periphery (position depicted by (↑) on the resection view in the *Top Left*) of the stemless humeral implant with respect to the humeral resection plane on a 135° NSA model. White markings on the bone (**A**) and implant (**B**) served as tracking points during micromotion measurement. The anterosuperior and anterior regions of interest relative to the resection plane view are indicated by (↑). *NSA*, neck shaft angle.

significantly higher in the 135° NSA implantations ($P < .001$) (135° NSA failures: total n = 6 [at load levels: 20%: 0, 40%: 0, 60%: 1, 80%: 3, 100%: 2], 145° NSA failures: total n = 3 [at load levels: 20%: 0, 40%: 0, 60%: 1, 80%: 0, 100%: 2]) (Fig. 7).

Discussion

The principal objective of this work was to evaluate the comparative biomechanical performance of a metaphyseal filling

Table I
Micromotion data during increasing cyclical load tests.

	Direction	20%	40%	60%	80%	100%
135°	Average	11 ± 4	35 ± 27	118 ± 93	100 ± 9	153 ± NaN
	Superior	16 ± 7	40 ± 18	138 ± 99	53 ± 16	74 ± NaN
	Anterior	10 ± 6	74 ± 103	80 ± 72	181 ± 205	None survived.
145°	Average	8 ± 6	23 ± 19	36 ± 27	69 ± 39	134 ± 114
	Superior	10 ± 3	25 ± 22	45 ± 47	85 ± 76	139 ± 100
	Anterior	6 ± 2	31 ± 27	37 ± 29	122 ± 76	234 ± 128

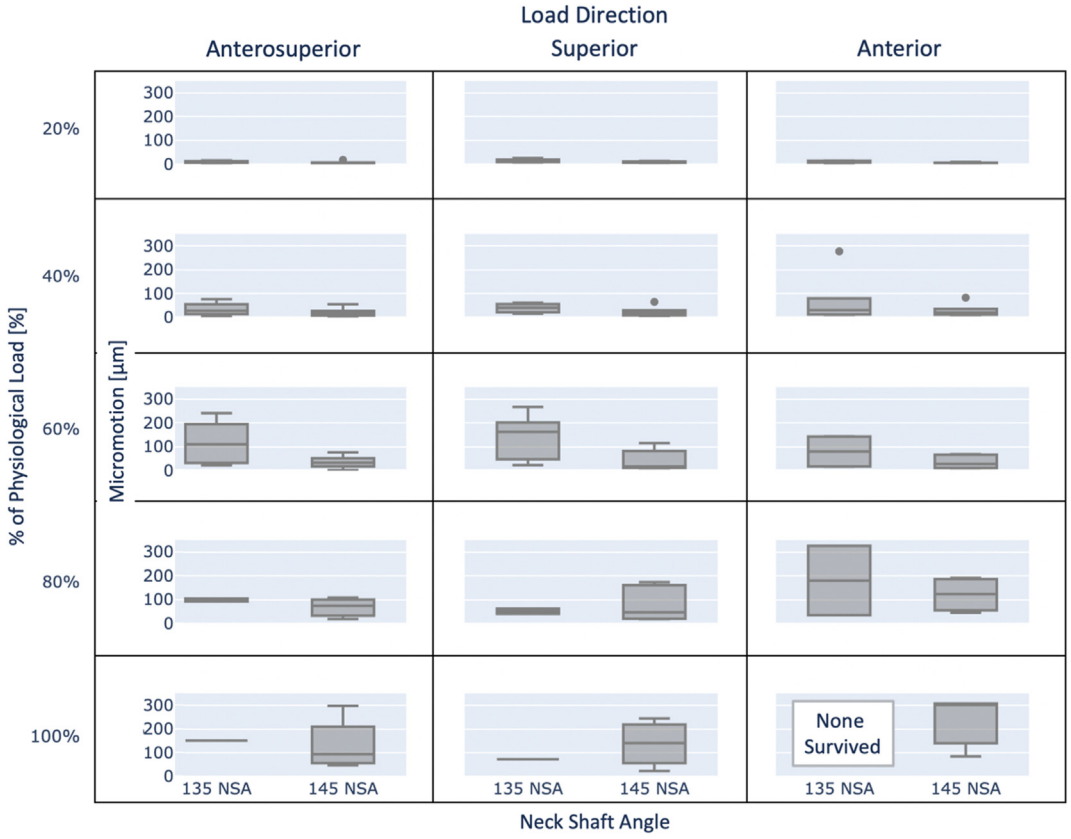

Figure 6 Micromotions developed in stemless reversed implants based on loading magnitude, NSA, and loading direction. Where an implant did not survive during a trial, it was given a micromotion of N/A and is not shown on the plot. *NSA*, neck shaft angle; *N/A*, not applicable.

2-tiered round stemless RSA humeral component implanted at 135° NSA and 145° NSA. We hypothesized that 145° NSA stemless pressfit implants would exhibit better primary fixation and biomechanical survivorship when compared to 135° NSA stemless pressfit implants. Our results identified that increasing NSA from 135° to 145° substantially increased time-zero stemless implant fixation and biomechanical survivorship. Additionally, the results indicated that when stemless humeral components are subjected to cyclical loading, critical implant fixation failure may occur when single-load distractive micromotions are well below the previous referenced limit of 150 μm for successful osseointegration.[2,3,9,14]

The osseointegrative potential of porous humeral stemless implants has not yet been thoroughly investigated, and existing studies evaluating the primary fixation of press-fit implants have defaulted to the literature, accepting the 150-μm threshold for osseointegration without fibrous tissue formation.[2,3,9,14] However, this threshold appears to be relevant to shear or tangential micromotion, commensurate with axially loaded stemmed implant designs. Indeed, previous reports have indicated that for ideal osseointegration, full contact between the implant and bone should be maintained, and any level of shear or distractive micromotion may potentially negatively influence the success of primary and secondary fixation.[20,22] The micromotions observed in this work show this threshold of long-term fixation surpassed even at 40% physiological load, which supports the directive of postoperative immobilization to increase the probability of successful long-term fixation.

Measurement of implant stability is a commonly utilized assessment method when evaluating the osseointegrative potential of different orthopedic implants.[2-4,8,9,17,21] The use of high-resolution digital tracking methods for the quantification of implant stability (viz micromotion) is becoming more widely utilized.[8,9] This technique is able evaluate the implant–bone interface during the application of loads that may realistically be experienced postoperatively during activities of daily living (ADLs).[6,7,16,25] Although the use of linear variable digital transformers has been commonly utilized in the experimental evaluation of shoulder implants,[2] it has previously been found that linear variable digital

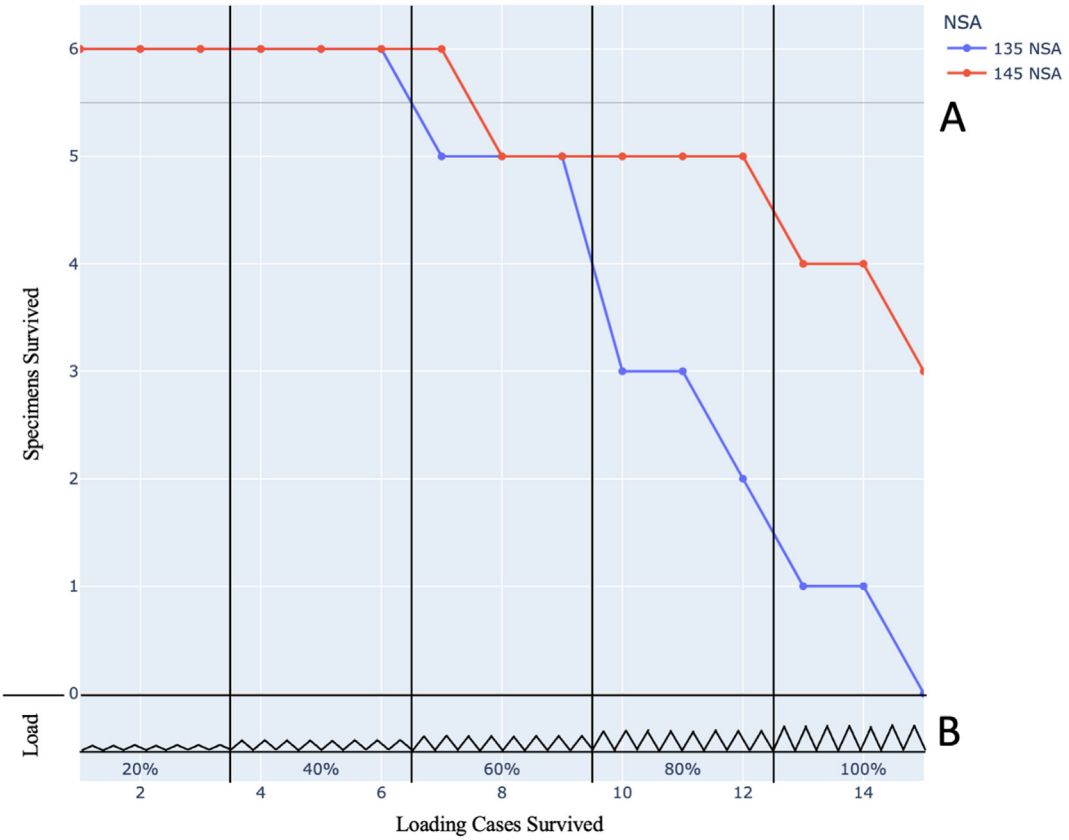

Figure 7 Survivability of stemless reversed implants based on NSA and cycles survived at increasing load magnitudes. The above plot (**A**) shows the number of specimens surviving at each loading case, whereas the below plot (**B**) shows a representation of the cyclical loading at increasing magnitudes. Please note that the plot in (**B**) is a representation of the cyclical loading, and in actuality, each specimen underwent a total of 90 cycles at each load level. *NSA*, neck shaft angle.

transformer methods may over-report implant–bone relative motion,[8] so a high-resolution digital tracking system was used.

Given the interface changes that were observed due to the loading states simulated, it is logical to postulate that loading of this nature may be an impediment to osseous integration and may contribute to early migration of subsidence if it were to occur postoperatively. When interpreting the telemetrized implant data available, there are only a limited number of activities that maintained load magnitudes of less than 40% of the physiological boundary load (53% body weight), and those ADLs identified as "safe" were limited to physiotherapist-assisted external rotation motions (in 1/1 patient(s)) and controlled unweighted 90° abduction motions (in 4/17 patient(s))[6] (Fig. 8). It is therefore reasonable to postulate that immobilization during the first 4 to 6 weeks after surgery may serve to decrease implant–bone micromotion, thereby increasing the potential for bone on-growth with resultant increased long-term fixation in stemless humeral implants. However, 4 to 6 weeks of sling use may result in increased joint stiffness, which may take longer to resolve. Previous investigations on the effect of modifying NSA have reported comparable results, indicating that lower, more varus NSAs exhibit lower levels of stability[5]; therefore also supporting the position that when implant stability is of concern, higher NSAs may improve early implant stability in stemless reverse humeral components.[5] Although both the 135° NSA and 145° NSA cohorts experienced failures, it is important to note that the conservative loads utilized for this work were intended to represent the worst-case conditions that a shoulder implant might experience postoperatively, before any osseointegration had occurred.

Increasing humeral component NSA, however, may have important negative implications, including decreased impingement-free range of motion in adduction,[24] increased risk of scapular notching,[13] increased humeral distalization, and possibly reduced internal/external rotation.[1,13] As such, it is important to consider all these factors when selecting an appropriate NSA. When using a traditional stemmed implant with diaphyseal or metadiaphyseal fixation, the effect of NSA on primary implant stability is likely less pronounced.

Implant fixation has frequently been studied in the shoulder, however, most studies have focused on glenoid components[2]; as such, there are limited protocols currently available for the evaluation of humeral component implant performance. In a clinical setting, humeral implants are subjected to a wide range of loading;[6] hence, it is reasonable to postulate that testing should include a comprehensive protocol. Most recently, studies have employed cyclical loading protocols to better mimic the early performance of uncemented devices[4,7,10]; a strategy that was also employed herein. Additionally, due to the diverse array of loading states that are experienced by the shoulder postoperatively, this study utilized a novel loading protocol that was designed to examine the fixation of implants using an increasingly aggressive loading protocol. This was important, as this study also aimed to assess the survivability of humeral implants during loading that best attempted to mimic the physiological state.

As discussed, one of the outcome measures leveraged in this work was distractive micromotion magnitude. This metric is most commonly associated with osseointegration, as bony ingrowth is generally more successful when implant micromotion is

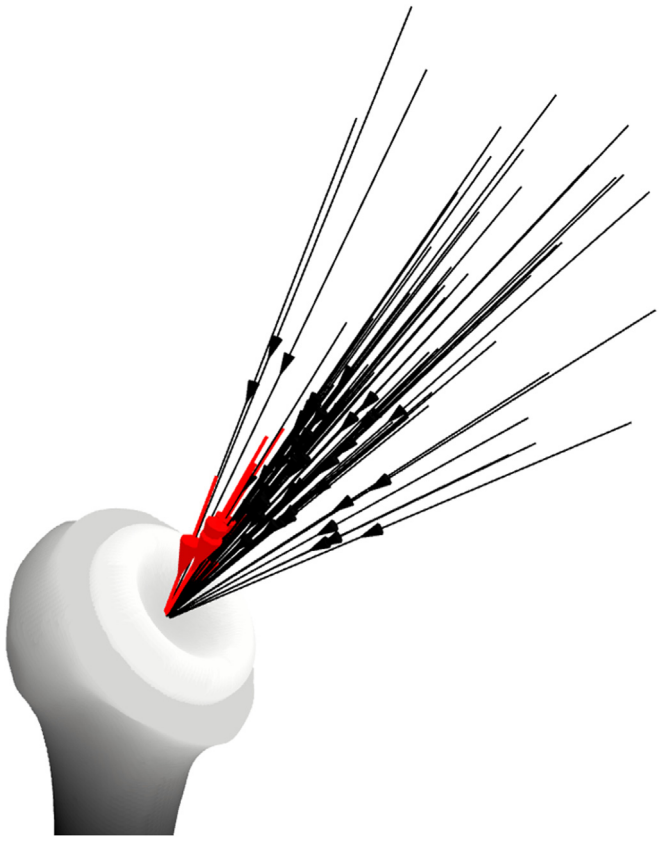

Figure 8 A 3D plot of the proximal humerus, showing all relevant OrthoLoad[6] activities used in the calculation of boundary loading limits in vector format. All (↑) represent ADLs that exceed the 40% physiological load survivorship limit determined by the study. The (↑) show the ADLs that were below the 40% limit. Only no-weight abduction and external rotation in 90° elbow flexion, supported by a physiotherapist were determined as "safe" activities in a few of the patients. *ADLs*, activities of daily living.

limited.[2,3,9,14] However, existing literature rarely differentiates between tangential (shear) and orthogonal (distractive) micromotion. In fact, to the authors' knowledge, there are no studies that examine the influence of cyclical loading on the osseointegration of surfaces resisting load in the distractive direction. As it has been proposed that the mechanism of implant–bone distractive fixation is dependent on the osseointegrated surface area and level of osseointegration,[19] this would imply that when the level of osseointegration is negligible, any loads resulting in distractive micromotions would not be resisted in the orthogonal direction by adhesion phenomena;[11] hence, osseous ingrowth in the distractive direction may be compromised by comparatively small micromotion magnitudes. This is noteworthy, as for implant geometries that rely on fixation to a primarily cancellous bone foundation, eccentric loading is known to cause "lift-off" and hence analyses of fixation in these constructs requires assessment of implant micromotion orthogonal to the interface. Previous finite element studies for the evaluation of micromotion in humeral implants found the primary mode of micromotion at the interface to be distractive micromotion for a similar implant geometry investigated.[7] Hence, distractive micromotion was utilized as the outcome measure of this work, but 150 μm was not purposed as a hard limit as knowledge on the relevance of that value is disputed. The experimental approaches employed herein have also been widely employed for tibial and glenoid implants.[2,14,21]

There are limitations with the present study. Primarily, boundary loading limits were established using in vivo telemetrized data for anatomic implants. This is noteworthy, as reversed implants are likely to experience lower magnitudes of articular force at potentially higher eccentricities due to the medialized center of rotation and increased deltoid moment arm.[15] However, for the purposes of this work, a conservative approach using larger magnitude loading was used as telemetrized data for RSA implants are not yet available.[5] This evaluation also focused on time-zero (directly after implantation) implant behaviors. As trabecular bone is a mechanoresponsive material and press-fit implants rely on osseointegration for fixation, stability during the postoperative rehabilitation period may differ in a clinical setting. Lastly, this evaluation only investigated 1 design of stemless RSA humeral implant. Future works should assess additional implant designs with a large variation in fixation geometry to provide a more thorough evaluation of the effect of NSA.

Conclusion

NSA in stemless reverse humeral components is a modifiable intraoperative parameter that significantly effects the time-zero stability and early survivorship of the stemless reverse humeral component implant design tested. The results demonstrate that a metaphyseal filling round 2-tiered stemless implant inserted at an NSA of 145° exhibits better primary stability than when inserted at 135° during simulated early postoperative physiological loading scenarios. It is suggested, therefore, with conditions of poorer humeral bone quality, that a higher, more valgus, NSA may be considered to maximize time-zero stemless implant fixation. Alternatively, sling immobilization to limit provocative ADLs in the early postoperative period will decrease undesirable bone-implant micromotions.

Acknowledgment

The authors acknowledge support provided by the Stryker Corporation, The Natural Sciences and Engineering Research Council of Canada, and the St. Joseph's Healthcare Roth McFarlane Hand and Upper Limb Centre, The University of Western Ontario, London, Ontario, Canada.

Disclaimers:

Funding: Implants donated by Stryker. No company had any input in to the experimentation, results, analysis or manuscript preparation.
Conflicts of interest: George S. Athwal is a consultant for Stryker, Conmed, and Exactech, and has received research support from Stryker. All the other authors, their immediate families, and any research foundations with which they are affiliated have not received any financial payments or other benefits from any commercial entity related to the subject of this article.

References

1. Arenas-Miquelez A, Murphy RJ, Rosa A, Caironi D, Zumstein MA. Impact of humeral and glenoid component variations on range of motion in reverse geometry total shoulder arthroplasty: a standardized computer model study. J Shoulder Elbow Surg 2021;30:763-71. https://doi.org/10.1016/j.jse.2020.07.026.
2. American Society for Testing and Materials (ASTM). F2028-17 Standard Test Methods for Dynamic Evaluation of Glenoid Loosening or Disassociation. ASTM. pp. 1-15, 2018. https://doi.org/10.1520/F2028-17.
3. Bonnevialle N, Geais L, Müller JH, Berhouet J. Effect of RSA glenoid baseplate central fixation on micromotion and bone stress. JSES Int 2020;4:979-86. https://doi.org/10.1016/j.jseint.2020.07.004.

4. Chen RE, Knapp E, Qiu B, Miniaci A, Awad HA, Voloshin I. Biomechanical comparison of stemless humeral components in total shoulder arthroplasty. Semin Arthroplasty JSES. 2021;32:145-53. https://doi.org/10.1053/j.sart.2021.08.003.
5. Cunningham DE, Spangenberg GW, Langohr GDG, Athwal GS, Johnson JA. Stemless reverse humeral component neck shaft angle has an influence on initial fixation. J Shoulder Elbow Surg 2024;33:164-71. https://doi.org/10.1016/j.jse.2023.06.035.
6. Damm P, Dymke J. Orthoload database . Jul. Wolff Inst. https://orthoload.com/database/.
7. Favre P, Henderson AD. Prediction of stemless humeral implant micromotion during upper limb activities. Clin Biomech 2016;36:46-51. https://doi.org/10.1016/j.clinbiomech.2016.05.003.
8. Favre P, Perala S, Vogel P, Fucentese SF, Goff JR, Gerber C, et al. In vitro assessments of reverse glenoid stability using displacement gages are misleading - Recommendations for accurate measurements of interface micromotion. Clin Biomech 2011;26:917-22. https://doi.org/10.1016/j.clinbiomech.2011.05.002.
9. Favre P, Seebeck J, Thistlethwaite PAE, Obrist M, Steffens JG, Hopkins AR, et al. In vitro initial stability of a stemless humeral implant. Clin Biomech 2016;32:113-7. https://doi.org/10.1016/j.clinbiomech.2015.12.004.
10. Freitag T, Kutzner KP, Bieger R, Reichel H, Ignatius A, Dürselen L. Biomechanics of a cemented short stem: a comparative in vitro study regarding primary stability and maximum fracture load. Arch Orthop Trauma Surg 2021;141:1797-806. https://doi.org/10.1007/s00402-021-03843-x.
11. Gao X, Fraulob M, Haïat G. Biomechanical behaviours of the bone-implant interface: a review. J R Soc Interface 2019;16:13-7. https://doi.org/10.1098/rsif.2019.0259.
12. Gobezie R, Shishani Y, Lederman E, Denard PJ. Can a functional difference be detected in reverse arthroplasty with 135° versus 155° prosthesis for the treatment of rotator cuff arthropathy: a prospective randomized study. J Shoulder Elbow Surg 2019;28:813-8. https://doi.org/10.1016/j.jse.2018.11.064.
13. Jeon BK, Panchal KA, Ji JH, Xin YZ, Park SR, Kim JH, et al. Combined effect of change in humeral neck-shaft angle and retroversion on shoulder range of motion in reverse total shoulder arthroplasty - a simulation study. Clin Biomech 2016;31:12-9. https://doi.org/10.1016/j.clinbiomech.2015.06.022.
14. Kohli N, Stoddart JC, van Arkel RJ. The limit of tolerable micromotion for implant osseointegration: a systematic review. Sci Rep 2021;11:10797. https://doi.org/10.1038/s41598-021-90142-5.
15. Langohr GD. Fundamentals of the biomechanical characteristics related to the loading of reverse total shoulder arthroplasty implants and the development of a wear simulation strategy [online]. 2015. Accessed May 1, 2023. https://ir.lib.uwo.ca/etd/3436/?utm_source=ir.lib.uwo.ca%2Fetd%2F3436&utm_medium=PDF&utm_campaign=PDFCoverPages.
16. Masjedi M, Johnson GR. Glenohumeral contact forces in reversed anatomy shoulder replacement. J Biomech 2010;43:2493-500. https://doi.org/10.1016/j.jbiomech.2010.05.024.
17. Quental C, Folgado J, Comenda M, Monteiro J, Sarmento M. Primary stability analysis of stemless shoulder implants. Med Eng Phys 2020;81:22-9. https://doi.org/10.1016/j.medengphy.2020.04.009.
18. Razfar N. Finite element modeling of the proximal humerus to compare stemless, short and standard stem humeral components of varying material stiffness for shoulder arthroplasty. Univ. West. Ontario - Electron. Thesis Diss. Repos 2014;2431. https://ir.lib.uwo.ca/etd/2431.
19. Rønold HJ, Ellingsen JE. The use of a coin shaped implant for direct in situ measurement of attachment strength for osseointegrating biomaterial surfaces. Biomaterials 2002;23:2201-9. https://doi.org/10.1016/S0142-9612(01)00353-2.
20. Sánchez E, Schilling C, Grupp TM, Giurea A, Wyers C, van den Bergh J, et al. The effect of different interference fits on the primary fixation of a cementless femoral component during experimental testing. J Mech Behav Biomed Mater 2021;113:104189. https://doi.org/10.1016/j.jmbbm.2020.104189.
21. Suárez DR, Nerkens W, Valstar ER, Rozing PM, van Keulen F. Interface micromotions increase with less-conforming cementless glenoid components. J Shoulder Elbow Surg 2012;21:474-82. https://doi.org/10.1016/j.jse.2011.03.008.
22. Viceconti M, Brusi G, Pancanti A, Cristofolini L. Primary stability of an anatomical cementless hip stem: a statistical analysis. J Biomech 2006;39:1169-79. https://doi.org/10.1016/j.jbiomech.2005.03.024.
23. Virtanen P, Gommers R, Oliphant TE, Haberland M, Reddy T, Cournapeau D, et al. SciPy 1.0: fundamental algorithms for scientific computing in Python. Nat Methods 2020;17:261-72. https://doi.org/10.1038/s41592-019-0686-2.
24. Werner BS, Chaoui J, Walch G. The influence of humeral neck shaft angle and glenoid lateralization on range of motion in reverse shoulder arthroplasty. J Shoulder Elbow Surg 2017;26:1726-31. https://doi.org/10.1016/j.jse.2017.03.032.
25. Zimmerman WF, Miller MA, Cleary RJ, Izant TH, Mann KA. Damage in total knee replacements from mechanical overload. J Biomech 2016;49:2068-75. https://doi.org/10.1016/j.jbiomech.2016.05.014.